Digital Discovery

ROYAL SOCIETY OF CHEMISTRY

PAPER

View Article Online
View Journal

Cite this: DOI: 10.1039/d6dd00007j

RobInHood: a robotic chemist in a fume hood

Louis Longley, Francisco Munguia-Galeano, Yushu Han, Rob Clowes, Sriram Vijayakrishnan, Adam Edwards, Gabriella Pizzuto, Hatem Fakhruldeen and Andrew Cooper *

Received 8th January 2026
Accepted 18th May 2026

DOI: 10.1039/d6dd00007j

rsc.li/digitaldiscovery

Fume hoods protect chemists and the environment from hazardous vapours and airborne substances produced during experiments. They are standard in chemistry laboratories worldwide. However, fume hoods were designed for manual chemistry, and there are still relatively few robotic systems designed to operate within these inherently confined spaces. It is challenging to design robotic systems that can perform the same variety of operations within fume hoods that can be performed by a dexterous human chemist. Here, we present an automated platform comprising a robotic arm that can perform liquid handling, solid handling, capping/decapping, heating and stirring, filtration, and sample imaging within a standard laboratory fume hood (50 cm × 120 cm × 170 cm). The broad applicability of this system was demonstrated in two materials research problems (a dye-based porosity screening workflow and the synthesis of a porous organic cage) and in a phthalimide synthesis. The success of the synthesis workflows was validated offline by NMR, X-ray diffraction, mass spectrometry and FTIR.

Introduction

There has been a major push recently toward automation and digitalisation of chemistry because of the benefits to speed and reproducibility that are possible with automatic sample preparation, data collection, and data analysis. Automation methods have been developed in many different areas of chemistry, including synthesis of small molecules,[1–3] organic cages,[4] polymers,[5] and materials,[6–8] as well as formulation[9] and characterisation.[10–13] There are many different reaction variables, such as temperature, atmosphere, solvent choice, and work-up conditions that must be automated in such chemical workflows. This has led to a plethora of different approaches ranging from flow chemistry,[14] static arms,[1,7,8] custom built assemblies,[15,16] commercial liquid handlers,[2,17] and mobile robots.[9,10,18]

Most manual chemical experiments are conducted inside fume hoods, which are the de facto standard worldwide. Fume hoods protect chemists from hazardous vapours and, in some experiments, airborne powders. Although the use of robots in laboratories can potentially alleviate such safety issues by removing humans from the laboratory, such fully automated setups are rare, expensive, and time consuming to build. Even in fully automated setups, humans would likely be needed to replenish reagents and to carry out repair and maintenance work—for example, to carry out routine scheduled testing of the fume hood extraction. Moreover, there is an enormous installed capital base of existing fume hoods worldwide, and the global fume hood market has been estimated to reach $1.9 billion USD by 2032.[19]

The Cronin group and collaborators[15,16,20] have worked extensively on incorporating automated workflows into standard laboratory fume hoods. Typically, reaction mixtures are moved between different stations by pumps and work-up and analysis occurs at these different stations. This approach has enabled many different synthesis and work-up procedures to be automated successfully.

Here, we propose a different approach—Robot-In-a-Fume-Hood (RobInHood) (Fig. 1)—in which a robot arm is integrated into a standard laboratory fume hood. The use of a robot arm allows multiple samples to be transported between different stations within vials enabling parallel sample preparation. RobInHood features solid and liquid dispensing, capping/decapping, stirring, heating, filtering, storage, and vision-based analysis, all within a compact fume hood space (50 cm × 120 cm × 170 cm). We demonstrate the versatility of RobInHood by using it to conduct three distinct workflows: a low-cost, high-speed porosity screen,[21] the synthesis a porous organic cage,[22,23] and the synthesis of a phthalimide.[24]

Results and discussion

Overview of the RobInHood station

The aim of the RobInHood set-up (Fig. 1) was to enable all the key unit operations in sample preparation and filtration to be conducted autonomously within a standard fume hood. A video of RobInHood in operation can be found in the raw data repository (Zenodo repository Video 1, https://youtu.be/VVtX8a-V6tc?si=71fI9Z4uT9UQ2YI8). The design philosophy of

Materials Innovation Factory, Department of Chemistry, University of Liverpool, Liverpool, L7 3NY, UK. E-mail: aicooper@liverpool.ac.uk

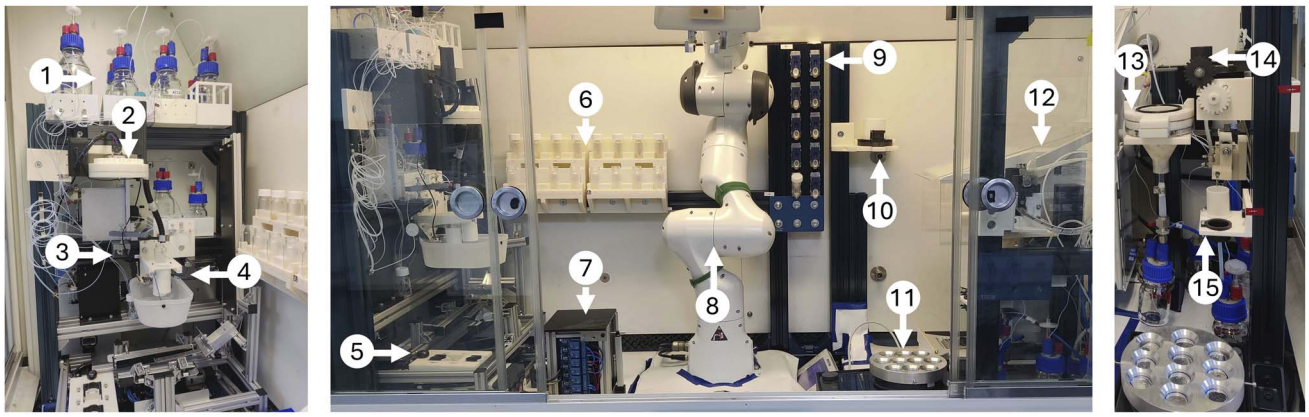

Fig. 1 The RobInHood platform. (A) Left side of the platform: 1. Liquid reagent storage. 2. The stirrer bar dispenser. 3. The syringe pumps and dispensing head. 4. The actuated vial holder and safety drip tray. (B) Centre of the platform: 5. The capper–decapper module. 6. Vial storage module. 7. Vision module/lightbox. 8. The Panda robotic arm. 9. Solid dispensing module (Quantos) cartridge storage. 10. Filtration cartridge storage. 11. Hot-plate. 12. Quantos solid dispenser. (C) Right side of the platform: 13. Filtration module receiving funnel and flask. 14. Filtration module pouring arm. 15. Filtration module receiving vial holder and dispensing head.

RobInHood leveraged the usable constrained working space of the robot by assigning it only to pick-and-place samples, quantos cartridges and filters, and using either existing hardware or constructing bespoke devices to carry out other operations such as liquid addition, stirrer bar dispensing, and capping/decapping. This approach improved the system's robustness. At the same time, this design philosophy reduced the number and complexity of routines that the robot needs to perform. To achieve this, the system was sub-divided into discrete modules, each of which provides one or more related functions:

(i) A seven-degree-of-freedom Emika Panda robotic arm (Franka), with custom designed fingertips, for sample vial, solid-dispensing and filter cartridge manipulation.
(ii) Vial storage module.
(iii) Liquid dispensing module.
(iv) Stirrer bar dispensing module.
(v) Capping/decapping module.
(vi) Solid dispensing module.
(vii) Heating and stirring module.
(viii) Vision-based analysis module.
(ix) Filtration module.

The system was mounted onto an aluminium frame secured against the sides of the fume hood using anchoring screws, preventing positional drift and increasing the reliability of robot motion. This aluminium profile structure allowed a smooth customisation and addition of devices within the station. For example, the usable vertical space was increased by attaching shelving units to the frame, constructed from aluminium extrusions. To further increase the reliability of the system custom fingers were added to the Panda. These were machined out of aluminium with concave fingertips 3D printed out of resin with rubber attached. These tips were designed to fit both the 20 ml vials and the Quantos cartridges used in the workflow (Fig. S1).

Adaptors were designed to allow for devices to be fixed in place relative to the frame (Fig. S2–S6). The liquid dispensing module, vision module, and filtration module are described in detail in the following sections. The vial storage consists of racks, printed out of ABS, designed to accommodate sixteen 20 mL vials (Fig. S4). The capper/decapper was custom-built to fit inside the tight space constraints of the fumehood (Fig. S7). A detailed description of the design is available in a related work;[25] briefly, the robot places a vial in either the capping or decapping lane and capping/decapping is achieved by friction between the cap and the rubber rail as the machine moves along a track. The solid dispensing module is comprised of a commercial Mettler Toledo Quantos, with a vial insert for repeatability of placement (Fig. S8), and a shelf with space for 10 solid dispensing cartridges (labelled 9 in Fig. 1B). The heating/stirring module was an RCT digital hotplate (IKA) with a custom aluminium heating block (Fig. S9) to allow the robot to place up to ten 20 mL vials onto the hotplate at once.

Liquid dispensing module

The liquid dispensing module (Fig. 1, 1–4) consists of two syringe pumps, an XCalibur (Tecan Cavro), and a C3000MP (TriContinent), nine reagent bottles, two waste vessels, an actuated vial holder (Fig. S10) and a stirrer bar dispenser (Fig. S11). During a liquid dispense, the robot arm places a vial in the vial holder, and an actuator then moves this vial below the dispense tubing, where liquid dispensing occurs, before returning the vial to the pick-up position. Two separate pumps are used due to issues encountered with high-vapour pressure solvents during preliminary testing, where it was observed that some intermixing of solvents in separate containers may occur through the pump valve. In the current system, these solvents can be handled on separate pumps that are fully isolated from one another. Pumps with valves made from two different materials, a ceramic (Tecan Cavro) and PCTFE (TriContinent),

were also chosen to broaden the solvent compatibility of the dispensing module.

At rest, the needle of the dispense module is positioned over a 40 mL waste vial to accommodate any overspill during washing and priming. The validity of the washing procedure was evaluated using methyl orange dye and UV-vis spectroscopy (SI Section 2.1.1). Once the needle has been primed, the identity of the priming solvent is stored in software so that the procedure is not repeated if another liquid dispense step using the same chemical is requested. Equally, if the user attempts to dispense a liquid without first priming it, the programme will display an error message. The accuracies of both pumps were measured using distilled water in the volume range (50–1000 μL) and found to be accurate (SI Section 2.1.2) under the dispensing conditions used in the workflow.

The liquid dispensing station can also be used to add stirrer bars to a sample. This feature was added because it was found that if samples were weighed with stirrer bars already present, then the magnetic field had an appreciable effect on the accuracy of the weighing (SI Section 2.2). The stirrer bar dispenser stores the stirrer bars in a carousel (Fig. S11). The vial holder closes a microswitch (Fig. S10-5) as the vial is moved under the needle, causing the carousel to be rotated *via* a Geneva wheel mechanism, and sending a stirrer bar down a chute and into the vial (Zenodo repository Video 2, https://youtube.com/shorts/k2w81RumC6A).

Vision module

The vision module used in RobInHood is a lightbox designed to work within the tight space confines of the system. The lightbox has a fish-eye lens camera (ELP USB camera module with 100° lens) and a white LED (Fig. S12). The fish-eye lens allows for taking pictures of the samples from a short distance (4 cm), thereby reducing the size of the box. The top is controlled with a linear actuator that, when it extends, causes a holder where the robot can put a vial to extend outward, and when it retracts closes the box, shutting out exterior light sources. Once the lid is closed, the LED light ensures consistent and uniform illumination of the samples.

Filtration module

Filtration is a crucial step in many workflows. Automated filtration *via* gravity filtering,[26] or *via* the addition of filter tips to liquid samplers[27] have both been reported previously in the literature. Here, we present a compact vacuum-assisted filtration module, analogous to Büchner filtration, capable of automatic liquid recovery, and where the solid phase remains accessible to manual recovery and analysis.

The filtration module consists of a vacuum filter set-up which has been adapted to be usable by the robotic arm (Fig. 1, 3–15). This consists of interchangeable filter-cartridges (Fig. 1, 10 and S13), a filter funnel (Fig. S14), a receiving flask (Fig. S15), a pouring arm (Fig. S16), a moveable output needle and a receiving vial holder for the filtrate vial (Fig. S17), a syringe pump (Tecan Cavro XCalibur), a waste container and system solvents for cleaning between samples (Fig. 1, 13–15). The actuators and vacuum generators are controlled by a pneumatics board and an electrical control box outside of the fume hood, with the pressure transmitting medium being compressed nitrogen that is built into the existing fume hood (Fig. S18 and S19).

The filter cartridges are made of three components (Fig. S13); a central filtering vessel, which has a splash guard and a rigid and smooth support plate for the filter papers/membranes, a surrounding collar, and handle to enable the cartridges to be moved by the robot, and a rubber gasket base that allows a vacuum seal to form between the filter cartridges and the filter funnel. The collar also contains notches, which key into locator fins on both the filter funnel and the holder, to facilitate consistent placement by the robot arm. Before use, the filter cartridges are manually loaded with a filter paper, which is held in place with an O-ring. Initially, the filtering vessel and collar were printed in white resin (Formlabs). This material was measured, using ^{1}H NMR, to be stable in water, with spectra remaining featureless apart from the D_2O peak,[28] even after 7 days of immersion (SI Section 2.3). These white resin filtering cartridges were used in the dye porosity screening workflow (see case studies). However, to facilitate broader solvent compatibility, subsequent filtering cartridges were produced in which the filtering vessel was made from PTFE. In this design, the collar is produced out of ABS by FDM printing, and the gasket is cast directly onto the base of the cartridge using a two-component liquid rubber.

The filter funnel is a glass funnel secured inside a 3D printed case (Fig. S14). This case allows the funnel to be supported from the fume hood frame and for a top plate, which can create an airtight seal between the funnel and the filter cartridge *via* an embedded O-ring. The opening between the bottom of the case and the stem of the glass funnel is made vacuum tight *via* an O-ring around the funnel stem.

The receiving flask is a 100 mL Schott Duran Flask, with three inputs integrated into the cap (Fig. S15). The first is a large PTFE tube (6 mm OD) connecting the receiving flask to the filter funnel, and the second is a PTFE tube connection (1.6 mm OD) to the syringe pump to enable filtrate recovery and cleaning. Finally, there is a connection to a pneumatic vacuum generator, which allows a vacuum to be generated in the receiving flask, increasing the driving force for filtering. The receiving flask is tilted to enable better recovery of the filtrate *via* the pump.

The pouring arm (Fig. S16) consists of a vial holder with a small pneumatic piston, which is used to clamp the vial in place during pouring, and a stepper motor, which is used to create the pouring motion. A small magnet attached to the vial holder is used to retain any stirrer bars inside the vial during pouring. Filtration can be operated for either a fixed time or in 'semi-manual' mode, where the process will continue indefinitely until a user input confirms that filtration has finished and restarts the workflow.

The workflow undertakes multiple steps during filtration, involving coordination of the Panda arm, liquid-dispensing module, capper–decapper and the filtration module itself (Fig. 2). The filtration process is divided into three stages: a pre-filtration wetting and cleaning stage, in which a vial of cleaning

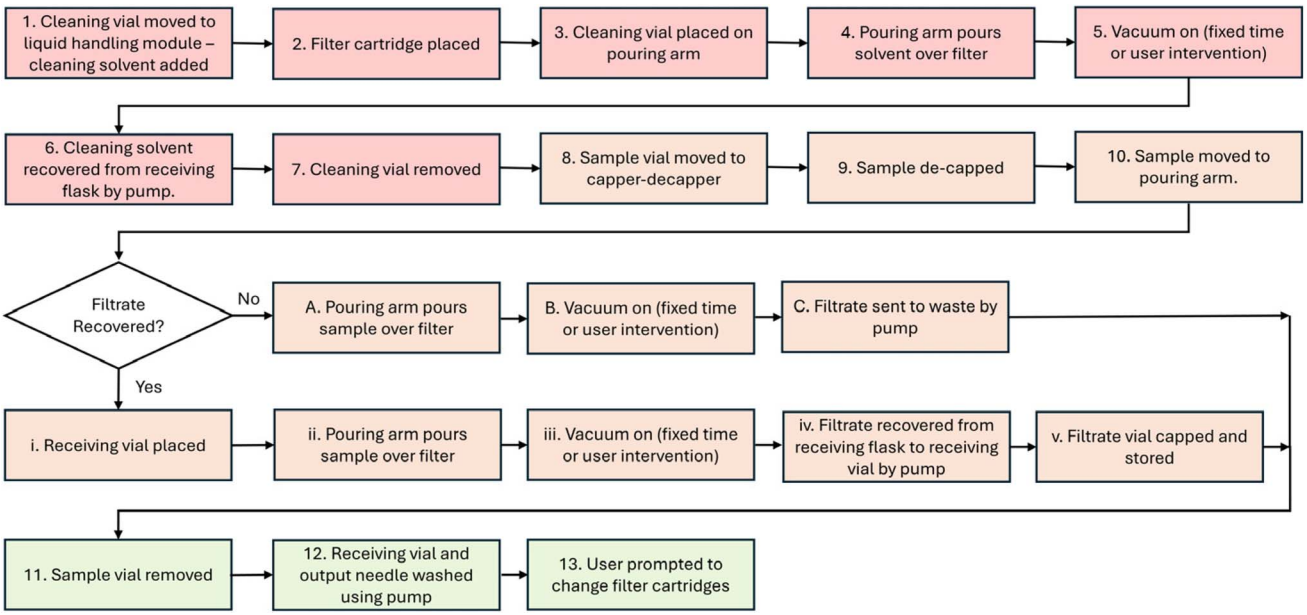

Fig. 2 The stages involved in sample processing in the sample filtration module. Numbered stages occur in all cases, whereas stages marked A–C and i–v occur only if the filtrate is discarded or recovered, respectively. Stages are classified as a pre-filtration, wetting, and cleaning (red), filtration (orange), and post-filtration cleaning (green).

solvent, the identity and volume of which is specified by the user, is used to wet the filter paper and clean the funnel. This is followed by a filtration stage, in which the sample vial is de-capped and then filtered. If the workflow specifies that the filtrate is needed for further analysis, then after filtration, the filtrate is recovered into a separate vial, otherwise it is sent straight to waste. Finally, a post-filtration cleaning stage occurs, where the receiving flask and output needle are washed with a wash-solvent also specified by the user. Currently, due to the confined nature of the station, there is only storage for a single filter cartridge, which must be manually changed by the user before the workflow continues (Fig. 2, 13). However, in principle, the method is easily extensible to multiple cartridges.

Software

The software that orchestrates the RobInHood operations is developed in Python, a user-friendly, popular, and powerful programming language that facilitates the integration of multiple advanced frameworks while also allowing the control of customised or commercial devices and labware. The integration of different commercial hardware (IKA Hotplate, Tecan Cavro XCalibur Pumps, Mettler Toledo Quantos *etc.*) is accomplished by drivers/wrappers written using the Pylabware framework,[29] whereas integration of electronic and pneumatic actuators and motors is achieved *via* serial communication between Python scripts and Arduino Uno boards embedded in each station. The Panda arm is controlled in Python using the FrankaX library[30] (Fig. 3). The full code-base for the station is available on Github (https://github.com/cooper-group-uol-robotics/RobInHoodPy).

Information about the chemicals stored in the workflow is contained in three .csv files. The dispense.csv file stores information about the liquids inside the liquid dispensing module, recording their chemical identity, the port of the dispensing pump that they are attached to, and any metadata entered by the user. The filt.csv file stores identical information for the liquid reagents connected to the pump in the filtration module. The quantos.csv file stores the chemical identity, position and metadata of solids in the solid dispensing module.

Information on the samples requested by the user from the workflow, solids to be added and in what amount, liquids to be added and in what volume, position of the sample vial, *etc.*, can be added as the samples.csv file. This file is converted into a dictionary, indexed by the order of the entries in the .csv file, when the workflow runs, which enables a large degree of flexibility in the order that samples can be prepared. Equally, information on the samples to be prepared can also be entered directly into the Python or Bash scripts.

RobInHood also uses these .csv files to cross-check that all reagents requested by the user in the samples.csv file are present in the workflow, reducing the potential for human error on setup. During workflow operation, the chemical identity of the solvents primed in each pump and the cartridge loaded into the Quantos is saved/stored as a JSON file, minimising time and reagent loss.

RobInHood-specific basic commands, such as moving vials from the vial rack to the hotplate or priming the reagent tubing in the liquid dispensing module, are written in a RobInHood class (Fig. S24). The methods in this class are then used to write scripts for individual workflows, with workflow-specific steps constructed from simpler pre-defined functions in the RobInHood class. These workflow steps are then called in the appropriate order within a Bash script, with pauses for the robot to read its own joint state, which we have observed improves the

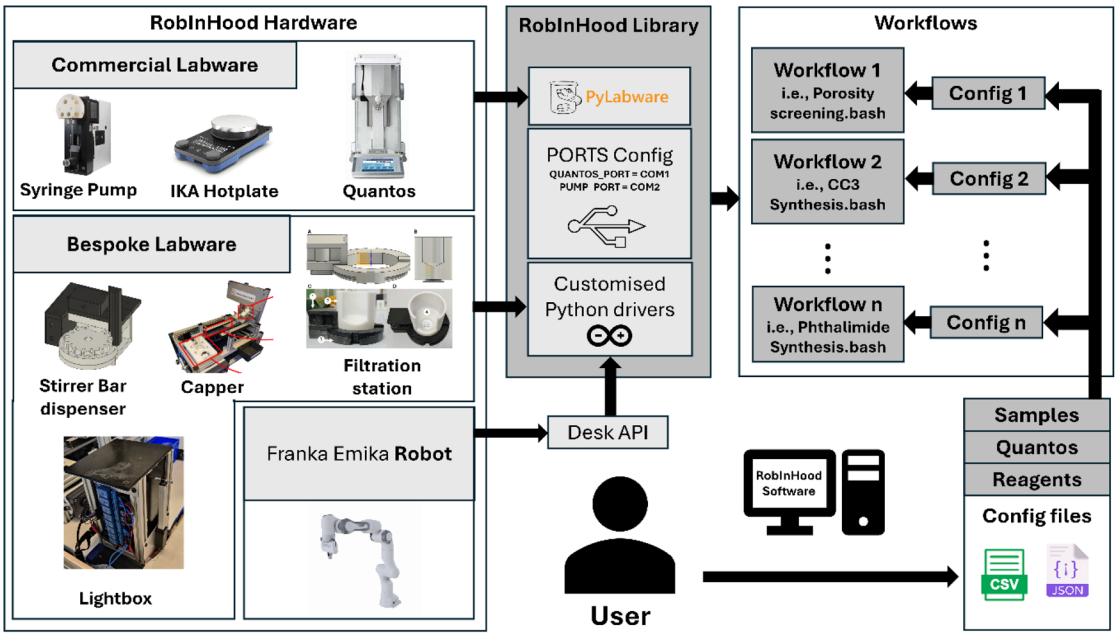

Fig. 3 Diagram showing the relationship between software and hardware in RobInHood. Python drivers (Pylabware and bespoke devices) are used to interface with devices. The Robinhood library/class stores station-specific methods and allows coordination of the different modules. Setup files (quantos, reagents and filtration) are used to specify the chemical identities of the liquid and solid reagents present in the system. User input occurs *via* the samples.csv files or variables directly entered in the workflow script.

reliability of the arm's motions. Once a workflow script has been written (GitHub https://github.com/cooper-group-uol-robotics/RobInHoodWorkflows), the composition of specific samples or identity of reagents can be easily altered by changing the relevant entries in the appropriate .csv files or *via* changing variables within the Bash script. This arrangement allows for a high degree of flexibility with different workflows being easily constructed from the same elementary commands.

Case studies

Case study 1: dye-based porosity screening. Porosity is an important property in functional materials research for applications such as in electrochemistry,[31] catalysis,[32] and chemical separations.[33,34] Standard porosity measuring techniques using gas sorption isotherms are precise but slow and difficult to adapt to autonomous workflows. To address this, we previously developed a qualitative high-throughput porosity screening workflow in which a material's ability to absorb an array of dye solutions was shown to be a useful proxy measurement for porosity.[21] This method measured the dye removal using a camera, which makes the process inexpensive and amenable to automation. However, unlike in gas-based porosity measurement techniques, the dye molecules themselves have distinct sizes and chemical structures, which can affect the extent of surface interactions and, hence, dye uptake from solution. As a result, an array of six dyes of varying size and structure was used instead of a single dye (dye 1 – lucifer yellow, dye 2 – ponceau xylidine, dye 3 – methyl orange, dye 4 – crystal violet, dye 5 – safranin o, dye 6 – acridine orange). Previous work on a variety of materials classes cross-validated with Brunauer–Emmett–Teller (BET) measurements[21] showed that colour loss in at least two of the six dyes indicated a porous sample. Here, colour loss was defined as a concentration of 1 ppm or below, where concentration is linked to colour through calibration of dye samples with known concentrations. The published work, performed previously by our group, was semi-automated, making use of a Quantos for solid dispensing, a Chemspeed Swing platform for dispensing the dye stock solutions, and manual filtration.

Here we successfully replicated the workflow in a fully autonomous fashion: empty vials were filled with the solid to be analysed (6 mg) using the Quantos, before 9 mL of the relevant dye and a stirrer bar was added in the liquid dispensing module. The vials were then capped and transferred to the stirrer plate for 24 hours before the filtration module was used to separate the solid from the dye solution. This filtered dye solution was transferred to a fresh vial, which was then capped and analysed in the vision module. After analysis, the vials were then transferred back to the vial rack for storage or disposal by the user. The process ran fully automatically from sample preparation to analysis. To increase throughput, the samples were sometimes transferred from the RobInHood hotplate to an external hotplate during the stirring process, allowing two sets of samples to be prepared simultaneously.

In our published work,[21] the dye-solid samples were manually filtered using syringe filtering to obtain the samples for analysis. Although syringe filtering is easy and effective for a trained human chemist, it presents multiple problems in an automated workflow: first, the procedure involves a high degree of manual dexterity, which is hard to translate to a robotic arm.

Second, the plunger can sometimes be removed unintentionally from the syringe, resulting in a dangerous, uncontrolled release of liquid, as a result of pressure building up while aspirating. Also, it is very difficult to recover the solid when syringe filtering, even when done manually, and this means that syringe filtering is not appropriate in many contexts. Therefore, as RobInHood was designed to be an adaptable general platform, we used vacuum filtration instead.

The validity of the fully automated workflow was tested by measuring the porosity of a subset of the materials measured in our original paper.[21] The selected materials included conjugated micropolymers (CMPs),[35] porous organic cages (POC)[36] and metal–organic frameworks (MOFs).[31] Additionally, we cross-calibrated our vision system by implementing the methodology presented in the SI (2.4 Dye based porosity screen calibration). Our results agree broadly with the findings of the original paper,[21] with the workflow correctly classifying all materials but one as porous or non-porous (Tables S6, S7 and SI Fig. S25–S31). The only sample where there was a discrepancy was CC19, which absorbed one dye (rather than two dyes[21]), which we ascribe to minor differences in calibration (Fig. 4).

Case study 2: synthesis of CC3. Porous organic cages are a broad class of molecular crystals.[36] The intrinsic porosity of these materials means that they can exhibit porosity in both the liquid and solid phase, and they are a promising materials class for use in absorption, gas separation, and catalysis.

CC3 is a prototypical example of porous organic cages[22] and has been studied widely. It is a tetrahedral cage composed of four benzene-1,3,5-tricarboxaldehyde (TFB) molecules linked by six 1,2-diaminocyclohexane molecules. The automated synthesis of CC3 was adapted from the literature.[23] Due to the low solubility of TFB in many solvents, 100 mg of solid TFB (0.62 mmol) was dispensed *via* the Quantos into each sample vial, illustrating one use for the solid dispensing module in RobInHood. The samples were then moved to the liquid handling module and received 2 mL of DCM that had been charged with a catalytic amount (0.013 mmol) of trifluoroacetic acid catalyst, before 2 mL of (1S, 2S)-(+)-1,2,-diaminocyclohexane (0.62 mmol) in DCM was added. The vials were then transferred to the capper, capped, and left to stand for 2 days, during which solid CC3 formed. The vials were then automatically decapped, and 8 mL of ethanol was added as an antisolvent to precipitate any CC3 that was still in solution. The contents of the vials were then filtered with the vial being transferred twice back to the

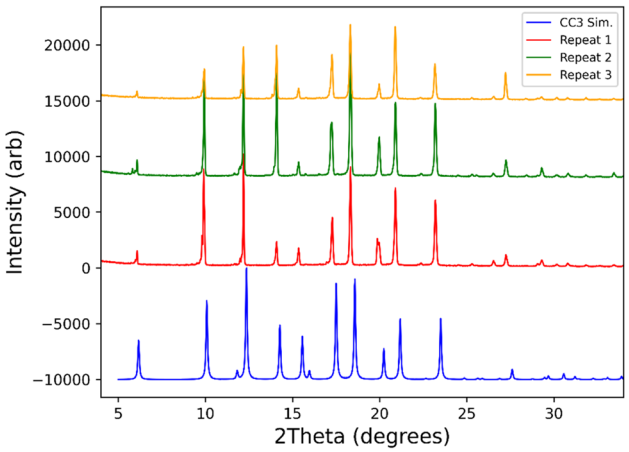

Fig. 5 PXRD patterns of three CC3 samples synthesised using RobInHood. The samples show good agreement with a calculated PXRD pattern based on the published structure for the alpha polymorph of CC3.[22] Differences in peak intensities for the three samples can be ascribed to preferred orientation; for example, a single large, oriented crystal can contribute disproportionately to the PXRD pattern.

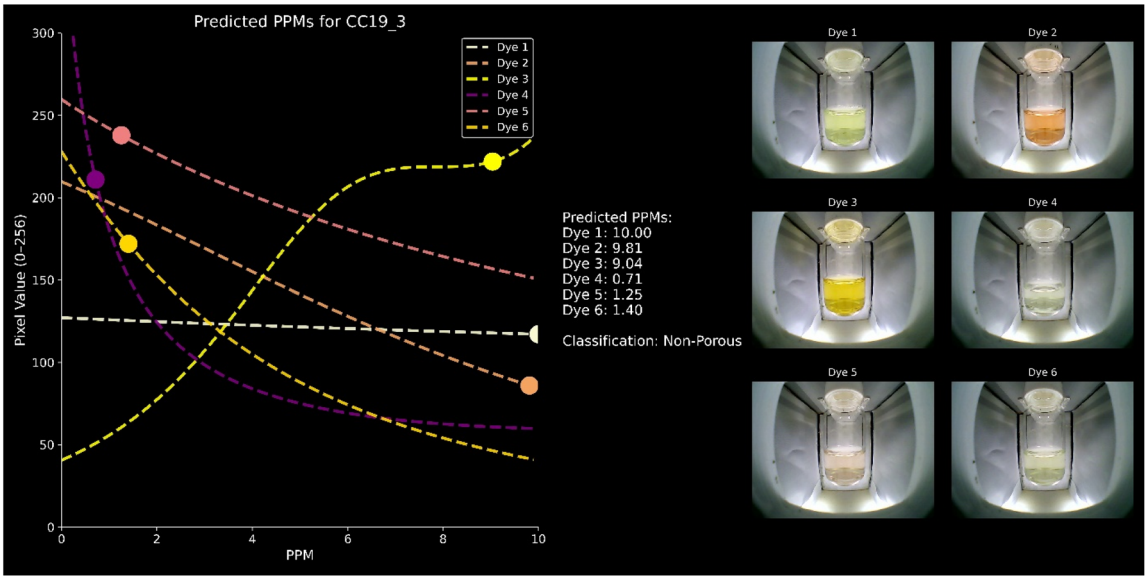

Fig. 4 Visual porosity results for CC19. Dye 4 is absorbed below the threshold of 1 ppm and therefore counts as porous, whereas dyes 1–3 and 5–6 remain above the threshold. The resulting material is classified as non-porous. However, in contrast to dyes 1–3, dyes 5–6 are heavily absorbing.

liquid dispensing module and refilled with 8 mL of 95% ethanol 5% DCM (vol/vol) before re-filtering to maximise product recovery. This step also had the dual purpose of washing the solid on the filter.

The solid was left to dry on the filter for approximately 12 hours before being recovered manually. The PXRD (Fig. 5), FTIR (Fig. S32) and ^{1}H NMR (Fig. S33) confirm the successful synthesis of the alpha polymorph of CC3,[22] with minor additional peaks in the PXRD and the additional hydrogens attached to sp^{3} carbons in the ^{1}H NMR being attributed to residual solvent and/or starting material resulting from incomplete activation of the cages.

Case study 3: synthesis of a phthalimide. Phthalimides are heterocyclic compounds that are imide derivatives of phthalic acid.[37] The phthalimide ring is a common scaffold for many biologically active molecules because of its hydrophobic aryl ring, combined with its hydrogen bonding capability and electron donor groups.[24,38] Phthalimide derivatives are commonly studied as potential active pharmaceutical ingredients with applications including antivirals, antibacterials and antitumour medications.[38] Phthalimide derivatives are commonly produced by either condensation of the phthalic acid anhydride or by alkylation of the imide nitrogen.

Here we produced a functionalised phthalimide by heating 4-nitrophthalic anhydride and 3,4-(methylenedioxy)aniline in acetic acid at 110 °C for 18 hours while stirring (Fig. 6A). The 4-nitrophthalic anhydride was added as a solid (193 mg, 1 mmol) using the Quantos solid dispenser. The vials were then transferred to the liquid handling station, and the aniline was added as a stock solution in acetic acid (9 mL, 1 mmol). During this step, a stirrer bar was also added to each sample. The samples were then capped and transferred to the hotplate. After heating, the samples were returned to the vial rack.

To aid product recovery, the samples were de-capped, and 6 mL of distilled water was added. These samples were then recapped and stirred for a further 20 minutes in the heating and stirring module. The samples were then de-capped again and filtered. After filtration, the samples were then washed with 2 × 10 mL of distilled water using the original sample vials in the same manner as the CC3 workflow. The product was allowed to dry on the filter for 12 hours before being collected manually. The success of the reaction was confirmed by ^{1}H NMR (Fig. 6B and S34), ^{13}C NMR and mass spectrometry (Fig. S35–S37). The yield and purity of this unoptimized reaction was consistent across each of the three repeats (24%, 23%, 24%) respectively.

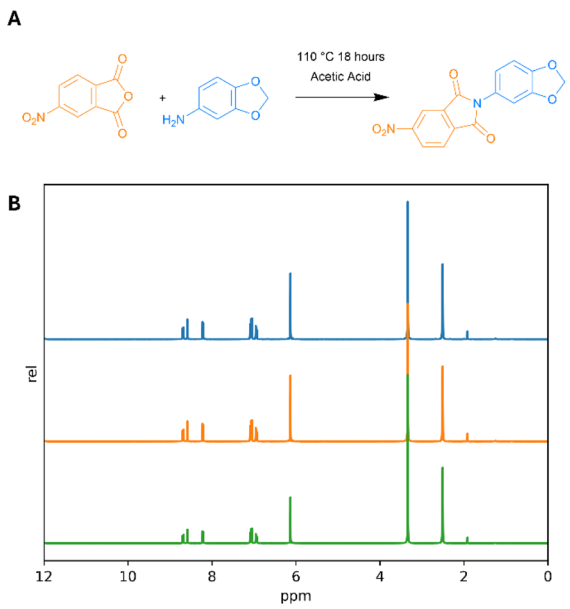

Fig. 6 (A) Reaction of 4-nitrophthalic anhydride and 3,4-(methylenedioxy)aniline to form the phthalimide using the RobInHood platform. (B) ^{1}H NMR (400 MHz, DMSO) spectra of phthalimide repeats. Additional peaks below 6 ppm, are 3.33 pm (H_2O), 2.5 ppm (d_6-DMSO), and 1.91 ppm (acetic acid – residual from synthesis).[28] For full spectra assignment see Fig. S34.

Conclusions and future work

This paper presents RobInHood, a generic synthesis and analysis system capable of liquid addition, solid addition, capping/decapping, heating/stirring, storage, visual analysis, and work-up by vacuum filtration. This system is fully contained within a standard laboratory fume hood and therefore has all the associated safety features, ventilation, fire suppression, and airflow monitoring. The system is controlled *via* Bash and/or Python scripting, enabling a high degree of user customisation and easy integration of data processing/storage. The broad applicability of the system was demonstrated *via* the successful completion of three diverse workflows; a dye-based high-throughput porosity analysis, the synthesis of a porous organic cage, and the synthesis of a phthalimide.

The use of a seven-degree-of-freedom arm as opposed to the more common Cartesian robot design in other automated chemistry platforms allows for a greater freedom of motion and, therefore, allows for the incorporation of more functionality into such a confined space. Moreover, the more human-like motion of the arm allows for easier adaptation of filtering and potentially other work-up procedures.

The small space available in the fume hood imposes limitations on the number of modules that can be implemented simultaneously, as well as the number of samples and reagents, which in turn limits the throughput and speed of the system. It also necessitates some manual intervention, for example, to change the filtration cartridges. However, despite these limitations, fume hoods are omnipresent in chemistry laboratories, and incorporating automation into these pre-existing chemically safe spaces represents a promising scalable alternative to augment existing standalone automation methods.

Nevertheless, additional modifications to fume hood design may make them easier to adapt to the needs of automation in the future. For example, fume hoods are not generally designed with consideration to communication with and between the devices contained within them; adding communication ports or cable channels would facilitate the implementation of automation in chemical settings while increasing safety. We believe that approaches such as the 'Internet of Things' will be adopted in the future by manufacturers, allowing easier implementation

and better system integration in the context of self-driving laboratories.

One key aspect of future work will focus on the automation of the fume hood door and the incorporation of a hand-off module, allowing samples to be passed into and out of the fume hood—for example, to a mobile robot. This feature would allow different fume hoods to be networked together, and for samples to be passed out of fume hoods for processing and analysis in larger bench-top or standalone instruments such as LC-MS or NMR.[18] To allow this, monitoring and safety systems[18,39] would need to be in place to ensure that the fume hood door was only opened when it was safe to do so, and closed in case of emergency.

Another key aspect of development is work to facilitate easier robot programming, *i.e.* involving the use of a digital twin,[40] which can be used to optimise the placement of submodules as well as to automatically generate the robot's waypoints, alongside the use of RGB-D cameras to align the physical and simulated environments. Additionally, such cameras, along with other sensors, could also be used to incorporate greater amounts of feedback, which would allow for more closed loop processes and automatic adjustments to workflows. Further software development could implement an AI agent as a workflow configuration helper that has knowledge of the platform's available features and could take user input and help suggest experiments compatible with the platform. The platform could also provide a user-friendly interface that more actively involves the user in the workflow decision-making process and lowers the barrier to entry for programming workflows. In the future, we imagine multiple RobInHood platforms in multiple networked fume hoods, each with its own specialisation, as a potentially scalable automation solution.

Author contributions

Conceptualisation, planning, and resource securing were done by LL, HF, GP and AIC. Automation, robotics, and station design were done and supervised by FMG and LL with assistance from RC. LL designed the automated filtration system with assistance from RC and FMG. The RobInHood software was written by FMG and LL with assistance from AE, while the pylabware drivers for the solid dispenser and syringe pumps were developed by LL. FMG designed and constructed the lightbox, stirrer bars dispenser, capper machine and the multipurpose fingers of the gripper with assistance from LL and wrote the customised drivers for these devices. The liquid dispensing station was designed and constructed by LL with assistance from FMG. FMG designed the cross-calibration method for the lightbox station. FMG and LL validated the robustness of RobInHood by performing repeated reliability trials and addressing all technical issues at the hardware and software levels through systematic troubleshooting with assistance from AE and RC. Case study 1 was developed by YH and its materials and stock solutions were also prepared by YH, case study 2 was developed by LL with assistance from YH, and case study 3 was developed by SV. Case study experiment workflows were written and supervised by LL with assistance from YH and SV. Offline analysis was conducted by YH, LL and SV. All authors provided feedback on the paper and the research.

Conflicts of interest

There are no conflicts to declare.

Data availability

The data supporting this article have been included as part of the supplementary information (SI). In addition to this the raw data from which these figures were produced, as well as CAD designs for the reproduction of the custom hardware, and videos of the station in operation are available in the following Zenodo repository: "Longley, L. (2026) 'RobInHood Raw Data and Hardware Designs'. Zenodo. https://doi.org/10.5281/zenodo.18183617". The GitHub containing the codebase referenced in the paper is available at the following URL: https://github.com/cooper-group-uol-robotics/RobInHoodPy. The GitHub containing the example workflows referenced in the paper is available in the following URL: https://github.com/cooper-group-uol-robotics/RobInHoodWorkflows. Device drivers utilised in the codebase are hosted on a private Cooper group repository but are available upon request. Supplementary information: module design, module calibration data, experimental methods, software structure and additional experimental results. See DOI: https://doi.org/10.1039/d6dd00007j.

Acknowledgements

This project was funded by the ERC ADAM Synergy grant (agreement no. 856405), the Engineering and Physical Sciences Research Council (EPSRC) under the grant agreement EP/V026887/1 and the Leverhulme Trust through the Leverhulme Research Centre for Functional Materials Design. A. I. C thanks the Royal Society for a Research Professorship (RSRP\S2\232003).

References

1 C. W. Coley, D. A. Thomas, J. A. M. Lummiss, J. N. Jaworski, C. P. Breen, V. Schultz, *et al.*, A robotic platform for flow synthesis of organic compounds informed by AI planning, *Science*, 2019, **365**(6453), eaax1566, DOI: 10.1126/science.aax1566.

2 W. Liu, J. Mulhearn, B. Hao, S. Cañellas, S. Last, J. E. Gómez, *et al.*, Enabling Deoxygenative C(sp ^{2})-C(sp ^{3}) Cross-Coupling for Parallel Medicinal Chemistry, *ACS Med. Chem. Lett.*, 2023, **14**(6), 853–859, DOI: 10.1021/acsmedchemlett.3c00118.

3 J. Li, S. G. Ballmer, E. P. Gillis, S. Fujii, M. J. Schmidt, A. M. E. Palazzolo, *et al.*, Synthesis of many different types of organic small molecules using one automated process, *Science*, 2015, **347**(6227), 1221–1226, DOI: 10.1126/science.aaa5414.

4 R. L. Greenaway, V. Santolini, M. J. Bennison, B. M. Alston, C. J. Pugh, M. A. Little, *et al.*, High-throughput discovery of organic cages and catenanes using computational screening fused with robotic synthesis, *Nat. Commun.*, 2018, **9**(1), 2849, DOI: 10.1038/s41467-018-05271-9.

5 H. Quinn, G. A. Robben, Z. Zheng, A. L. Gardner, J. G. Werner and K. A. Brown, PANDA: a self-driving lab for studying electrodeposited polymer films, *Mater. Horiz.*, 2024, **11**(21), 5331–5340, DOI: 10.1039/d4mh00797b.

6 T. C. Wu, A. Aguilar-Granda, K. Hotta, S. A. Yazdani, R. Pollice, J. Vestfrid, *et al.*, A Materials Acceleration Platform for Organic Laser Discovery, *Adv. Mater.*, 2023, **35**(6), 2207070, DOI: 10.1002/adma.202207070.

7 M. Zaki, C. Prinz and B. Ruehle, A Self-Driving Lab for Nano- and Advanced Materials Synthesis, *ACS Nano*, 2025, **19**(9), 9029–9041, DOI: 10.1021/acsnano.4c17504.

8 M. Omidvar, H. Zhang, A. A. Ihalage, T. G. Saunders, H. Giddens, M. Forrester, *et al.*, Accelerated discovery of perovskite solid solutions through automated materials synthesis and characterization, *Nat. Commun.*, 2024, **15**(1), 6554, DOI: 10.1038/s41467-024-50884-y.

9 B. Burger, P. M. Maffettone, V. V. Gusev, C. M. Aitchison, Y. Bai, X. Wang, *et al.*, A mobile robotic chemist, *Nature*, 2020, **583**(7815), 237–241, DOI: 10.1038/s41586-020-2442-2.

10 A. M. Lunt, H. Fakhruldeen, G. Pizzuto, L. Longley, A. White, N. Rankin, *et al.*, Modular, multi-robot integration of laboratories: an autonomous workflow for solid-state chemistry, *Chem. Sci.*, 2024, **15**(7), 2456–2463, DOI: 10.1039/d3sc06206f.

11 D. Milsted, T. P. Mishra, L. N. Walters, Y. Fei, B. Rendy, P. Nevatia, *et al.*, Automated electron microscopy sample preparation system, *Digital Discovery*, 2025, **4**(8), 2244–2252, DOI: 10.1039/D5DD00116A.

12 M. Walker, G. Pizzuto, H. Fakhruldeen and A. I. Cooper, Go with the flow: deep learning methods for autonomous viscosity estimations, *Digital Discovery*, 2023, **2**(5), 1540–1547, DOI: 10.1039/D3DD00109A.

13 E. M. Chan, C. Xu, A. W. Mao, G. Han, J. S. Owen, B. E. Cohen, *et al.*, Reproducible, high-throughput synthesis of colloidal nanocrystals for optimization in multidimensional parameter space, *Nano Lett.*, 2010, **10**(5), 1874–1885, DOI: 10.1021/nl100669s.

14 A. Slattery, Z. Wen, P. Tenblad, J. Sanjosé-Orduna, D. Pintossi, H. T. Den, *et al.*, Automated self-optimization, intensification, and scale-up of photocatalysis in flow, *Science*, 2024, **383**(6681), eadj1817, DOI: 10.1126/science.adj1817.

15 D. Angelone, A. J. S. Hammer, S. Rohrbach, S. Krambeck, J. M. Granda, J. Wolf, *et al.*, Convergence of multiple synthetic paradigms in a universally programmable chemical synthesis machine, *Nat. Chem.*, 2021, **13**(1), 63–69, DOI: 10.1038/s41557-020-00596-9.

16 J. S. Manzano, W. Hou, S. S. Zalesskiy, P. Frei, H. Wang, P. J. Kitson, *et al.*, An autonomous portable platform for universal chemical synthesis, *Nat. Chem.*, 2022, **14**(11), 1311–1318, DOI: 10.1038/s41557-022-01016-w.

17 M. Ringleb, A. Eith, S. Zechel, U. Schubert, K. Jablonka, J. Schneidewind, Kinetically guided exploration of photocatalytic reactions by combining automation with in situ measurements [Internet]. Chemistry, 2025, cited 2025 Aug 7, DOI: 10.26434/chemrxiv-2025-s9txt, available from https://chemrxiv.org/engage/chemrxiv/article-details/688a3057728bf9025e2028b1.

18 T. Dai, S. Vijayakrishnan, F. T. Szczypiński, J. F. Ayme, E. Simaei, T. Fellowes, *et al.*, Autonomous mobile robots for exploratory synthetic chemistry, *Nature*, 2024, **635**(8040), 1–8, DOI: 10.1038/s41586-024-08173-7.

19 R. Sharma, S. Bhat and V. Chandola, *Laboratory Fume Hoods Market Research Report 2033*, [Market Outlook] [Internet], Data Intelo, 2024, p. 261, available from https://dataintelo.com/report/global-laboratory-fume-hoods-market.

20 N. L. Bell, F. Boser, A. Bubliauskas, D. R. Willcox, V. S. Luna and L. Cronin, Autonomous execution of highly reactive chemical transformations in the Schlenkputer, *Nat. Chem. Eng.*, 2024, **1**(2), 180–189, DOI: 10.1038/s44286-023-00024-y.

21 Y. Han, I. Borne, B. Dutta, R. Clowes, H. Qu, A. James, *et al.*, Accelerated Porosity Screening Using a Multichannel Colorimetric Array, *Angew. Chem., Int. Ed.*, 2025, **137**(40), e202510400, DOI: 10.1002/anie.202510400.

22 T. Tozawa, J. T. A. Jones, S. I. Swamy, S. Jiang, D. J. Adams, S. Shakespeare, *et al.*, Porous organic cages, *Nat. Mater.*, 2009, **8**(12), 973–978, DOI: 10.1038/nmat2545.

23 M. E. Briggs and A. I. Cooper, A Perspective on the Synthesis, Purification, and Characterization of Porous Organic Cages, *Chem. Mater.*, 2017, **29**(1), 149–157, DOI: 10.1021/acs.chemmater.6b02903.

24 M. Kaur, S. Sharma and D. Utreja, A Review on Drug Discovery of Phthalimide Analogues as Emerging Pharmacophores: Synthesis and Biological Potential, *ChemistrySelect*, 2025, **10**(16), e202405580, DOI: 10.1002/slct.202405580.

25 F. Munguia-Galeano, L. Longley, S. Veeramani, Z. Zhou, R. Clowes, H. Fakhruldeen, *et al.*, An Open-Source Capping Machine Suitable for Confined Spaces, in *Towards Autonomous Robotic Systems*, ed. A. Cavalcanti, S. Foster, R. Richardson, Springer Nature Switzerland, Cham, 2026, pp. 461–474.

26 S. Neubert, S. Junginger, T. Roddelkopf, S. J. Burgdorf, N. Stoll and K. Thurow, Automated System for Pouring and Filtration Tasks in Laboratory Applications, *Chem.-Ing.-Tech.*, 2022, **94**(4), 530–541, DOI: 10.1002/cite.202000225.

27 A. J. Kukor, M. A. Guy, J. M. Hawkins and J. E. Hein, A robust new tool for online solution-phase sampling of crystallizations, *React. Chem. Eng.*, 2021, **6**(11), 2042–2049, DOI: 10.1039/D1RE00284H.

28 G. R. Fulmer, A. J. M. Miller, N. H. Sherden, H. E. Gottlieb, A. Nudelman, B. M. Stoltz, *et al.*, NMR chemical shifts of trace impurities: Common laboratory solvents, organics, and gases in deuterated solvents relevant to the organometallic chemist, *Organometallics*, 2010, **29**(9), 2176–2179, DOI: 10.1021/om100106e.

29 Pylabware [Github Repository], Pylabware, [Internet], cited 2025 Sep 3, available from https://github.com/croningp/pylabware.
30 Frankx [Github Repository], Frankx, [Internet], cited 2025 Dec 10, available from https://github.com/pantor/frankx.
31 V. F. Yusuf, N. I. Malek and S. K. Kailasa, Review on Metal–Organic Framework Classification, Synthetic Approaches, and Influencing Factors: Applications in Energy, Drug Delivery, and Wastewater Treatment, *ACS Omega*, 2022, **7**(49), 44507–44531, DOI: 10.1021/acsomega.2c05310.
32 K. A. Sanoja-López and R. Luque, Porous Materials for the Heterogeneously Catalyzed Synthesis of High Value-Added Products: Latest Trends and Future Prospects, *Chem.–Asian J.*, 2025, **20**(2), e202401238, DOI: 10.1002/asia.202401238.
33 Y. Song, J. Phipps, C. Zhu and S. Ma, Porous Materials for Water Purification, *Angew. Chem., Int. Ed.*, 2023, **62**(11), e202216724, DOI: 10.1002/anie.202216724.
34 Y. Wu and B. M. Weckhuysen, Separation and Purification of Hydrocarbons with Porous Materials, *Angew. Chem., Int. Ed.*, 2021, **60**(35), 18930–18949, DOI: 10.1002/anie.202104318.
35 J. S. M. Lee and A. I. Cooper, Advances in Conjugated Microporous Polymers, *Chem. Rev.*, 2020, **120**(4), 2171–2214, DOI: 10.1021/acs.chemrev.9b00399.
36 X. Yang, Z. Ullah, J. F. Stoddart and C. T. Yavuz, Porous Organic Cages, *Chem. Rev.*, 2023, **123**(8), 4602–4634, DOI: 10.1021/acs.chemrev.2c00667.
37 N. Kushwaha and D. Kaushik, Recent Advances and Future Prospects of Phthalimide Derivatives, *J. Appl. Pharm. Sci.*, 2016, **6**(3), 159–171, DOI: 10.7324/japs.2016.60330.
38 G. F. S. Fernandes, J. R. Lopes, J. L. Dos Santos and C. B. Scarim, Phthalimide as a versatile pharmacophore scaffold: Unlocking its diverse biological activities, *Drug Dev. Res.*, 2023, **84**(7), 1346–1375, DOI: 10.1002/ddr.22094.
39 S. X. Leong, C. E. Griesbach, R. Zhang, K. Darvish, Y. Zhao, A. Mandal, *et al.*, Steering towards safe self-driving laboratories, *Nat. Rev. Chem.*, 2025, **9**(10), 707, DOI: 10.1038/s41570-025-00747-x.
40 K. Darvish, A. Sohal, A. Mandal, H. Fakhruldeen, N. Radulov, Z. Zhou, *et al.*, MATTERIX: toward a digital twin for robotics-assisted chemistry laboratory automation, *Nat. Comput. Sci.*, 2026, **6**(1), 67–82, DOI: 10.1038/s43588-025-00924-4.